

The elaborated computed program is very general. It is very easy to increase the number of modes, to choose structures with n dielectric media, and to analyze anisotropic lines.

ACKNOWLEDGMENT

The computations used for this analysis have been made in the Computer Center of the University of Limoges.

REFERENCES

- [1] S. A. Schelkunoff, "Generalized telegraphists' equations for waveguides," *Bell System Tech. J.*, vol. 31, pp. 784-801, 1952.
- [2] W. E. Hord and F. J. Rosenbaum, "Approximation technique for dielectric loaded waveguides," *IEEE Trans. Microwave Theory Tech.*, vol. MTT-16, pp. 228-233, April 1968.
- [3] R. M. Arnold and F. J. Rosenbaum, "Nonreciprocal wave propagation in semiconductor loaded waveguides in the presence of a transverse magnetic field," *IEEE Trans. Microwave Theory Tech.*, vol. MTT-19, pp. 57-65, Jan. 1971.
- [4] —, "An approximate analysis of dielectric ridge loaded waveguide," *IEEE Trans. Microwave Theory Tech.*, vol. MTT-20, pp. 699-701, Oct. 1972.
- [5] J. B. Ness and M. W. Gunn, "Microwave propagation in rectangular waveguide containing a semiconductor subject to a transverse magnetic field," *IEEE Trans. Microwave Theory Tech.*, vol. MTT-23, pp. 767-772, Sept. 1975.

Dispersion in Shielded Planar Transmission Lines on Two-Layer Composite Substrate

P. K. SAHA

Abstract—The singular integral equation technique has been used to analyze a shielded planar transmission line, which allows one to calculate the dispersion characteristics of shielded microstrips on two-layer substrates as well as the effect of shielding on coplanar waveguides. Dispersion curves for suspended substrate microstrips and the variation of the relative phase velocity, with frequency, of coplanar waveguide (CPW) on alumina substrates of finite thicknesses and variable ground plane positions are presented. The results of computations with the lowest order 4×4 determinant show good agreement with the available data.

I. INTRODUCTION

THE theoretical analysis as well as the experimental investigation of the frequency dependent behavior of various planar transmission lines has received considerable attention in recent years [1]-[9]. These include shielded and unshielded microstrip lines and their derivatives such as slot lines, CPW, and coplanar strips on both infinite and finite dielectric substrates. However, not much information is available for dispersion in shielded microstrips on composite substrates. Hasegawa [10] and Guckel [11] have studied the open microstrips on composite substrates of finite conductivity using the parallel-plate waveguide model. Krage and Haddad [4] have presented the dispersion characteristics of single and coupled microstrips with overlay dielectric and of coupled microstrips on composite substrate, but, unfortunately, have not given any data on single microstrip on two-layer substrate. This author has used the singular integral equation technique of Mittra and

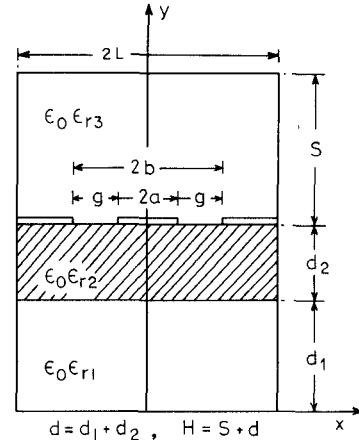


Fig. 1. Shielded coplanar waveguide.

Itoh [6] to study the dispersion characteristics of shielded single microstrips on composite substrates. The structure has been further modified by introducing two symmetrical coplanar ground planes (Fig. 1) so that the same analysis enables one to calculate the effect of shielding on dispersion in CPW on a finite substrate. Since the completion of the present work the author came across the recent work of Yamashita and Atsuki [12], who have analyzed similar structures by nonuniform discretization of integral equations.

Since the basic technique is the same as in [6], many steps in the mathematical derivation are omitted, and only the new relations necessary for computation are given explicitly. Results are presented in the form of normalized dispersion curves for the dominant modes only, although the higher

Manuscript received June 21, 1976; revised December 28, 1976.

The author is with the Institute of Radio Physics and Electronics, University College of Science and Technology, Calcutta, India.

modes can be extracted easily by seeking the higher roots of a 4×4 determinant.

II. ANALYSIS

Referring to the structure shown in Fig. 1, the modes with even symmetry ($H_z = \text{odd}$ and $E_z = \text{even}$) in x are considered. These are derivable from the appropriate scalar potentials $\psi_i^{(e)}$ and $\psi_i^{(h)}$, $i = 1, 2, 3$, through well-known relations. In view of the boundary conditions on the walls and the symmetry of the modes, the scalar potentials are written as

$$\psi_1^{(e)} = \sum_{n=1}^{\infty} A_n^{(e)} \cos \hat{k}_n x \sinh \alpha_{n1} y, \quad 0 < y < d_1$$

$$\psi_1^{(h)} = \sum_{n=1}^{\infty} A_n^{(h)} \sin \hat{k}_n x \cosh \alpha_{n1} y, \quad 0 < y < d_1 \quad (1)$$

$$\psi_2^{(e)} = \sum_{n=1}^{\infty} \cos \hat{k}_n x (B_n^{(e)} \sinh \alpha_{n2} y + C_n^{(e)} \cosh \alpha_{n2} y), \quad d_1 < y < d$$

$$\psi_2^{(h)} = \sum_{n=1}^{\infty} \sin \hat{k}_n x (B_n^{(h)} \cosh \alpha_{n2} y + C_n^{(h)} \sinh \alpha_{n2} y), \quad d_1 < y < d \quad (2)$$

$$\psi_3^{(e)} = \sum_{n=1}^{\infty} E_n^{(e)} \cos \hat{k}_n x \sinh \alpha_{n3} (H - y), \quad d < y < H$$

$$\psi_3^{(h)} = \sum_{n=1}^{\infty} E_n^{(h)} \sin \hat{k}_n x \cosh \alpha_{n3} (H - y), \quad d < y < H \quad (3)$$

where

$$\begin{aligned} \hat{k}_n &= (2n - 1)\pi/2L & k_0 &= \omega \sqrt{\mu_0 \epsilon_0} & \bar{\beta} &= \beta/k_0 \\ \alpha_{ni}^2 &= (\hat{k}_n^2/k_0^2 + \bar{\beta}^2 - \epsilon_{ri})k_0^2 = \hat{k}_n^2 - k_{ci}^2, & i &= 1, 2, 3 \end{aligned} \quad (4)$$

and the coefficients A_n , B_n , C_n , E_n are as yet unknown.

Applying the continuity of the total hybrid mode fields E_z , H_z , E_x , H_x at the first interface ($y = d_1$, $0 < x < L$) and eliminating $A_n^{(e)}$ and $A_n^{(h)}$, two sets of equations for four unknowns $\bar{B}_n^{(e)}$, $\bar{C}_n^{(e)}$, $\bar{B}_n^{(h)}$, and $\bar{C}_n^{(h)}$ are obtained, where

$$\begin{aligned} \bar{B}_n^{(e)} &= B_n^{(e)} \sinh \alpha_{n2} d & \bar{C}_n^{(e)} &= C_n^{(e)} \cosh \alpha_{n2} d \\ \bar{B}_n^{(h)} &= \frac{\omega \mu_0}{\beta} \frac{\alpha_{n2}}{\hat{k}_n} B_n^{(h)} \sinh \alpha_{n2} d \\ \bar{C}_n^{(h)} &= \frac{\omega \mu_0}{\beta} \frac{\alpha_{n2}}{\hat{k}_n} C_n^{(h)} \cosh \alpha_{n2} d. \end{aligned} \quad (5)$$

From the boundary conditions at the second interface ($y = d_1 + d_2 = d$), two pairs of equations are obtained the formal solutions of which are as follows:

$$\begin{aligned} \hat{k}_n \bar{B}_n^{(e)} + \hat{k}_n \bar{C}_n^{(e)} &= \sum_{m=1}^{\infty} (a_m \bar{B}_m^{(e)} + b_m \bar{B}_m^{(h)} + h_m \bar{C}_m^{(e)} + e_m \bar{C}_m^{(h)}) D_{nm} + \bar{r}_1 K_n, \\ n &= 1, 2, 3, \dots \end{aligned} \quad (6)$$

$$\begin{aligned} \hat{k}_n \bar{B}_n^{(h)} + \hat{k}_n \bar{C}_n^{(h)} &= \sum_{m=1}^{\infty} (c_m \bar{B}_m^{(e)} + d_m \bar{B}_m^{(h)} + q_m \bar{C}_m^{(e)} + p_m \bar{C}_m^{(h)}) D_{nm} + \bar{r}_2 K_n, \\ n &= 1, 2, 3, \dots \end{aligned} \quad (7)$$

where

$$\begin{aligned} a_m &= \hat{k}_m [1 - (Q_m T - P_m W)/\Delta] \\ b_m &= \hat{k}_m [W_m T - T_m W]/\Delta \\ h_m &= \hat{k}_m [1 - (Q_m T - G_m W)/\Delta] \\ e_m &= \hat{k}_m [R_m T - H_m W]/\Delta \\ c_m &= \hat{k}_m [P_m Q - Q_m P]/\Delta \\ d_m &= \hat{k}_m [1 - (T_m Q - W_m P)/\Delta] \\ q_m &= \hat{k}_m [G_m Q - Q_m P]/\Delta \\ p_m &= \hat{k}_m [1 - (H_m Q - R_m P)/\Delta] \end{aligned} \quad (8)$$

$$\begin{aligned} P_m(\beta) &= \epsilon_{r3} r_{23} \frac{\alpha_{m3}}{\hat{k}_m} \coth \alpha_{m3} S + \bar{\beta}^2 (1 - r_{23}) \frac{\hat{k}_m}{\alpha_{m3}} \coth \alpha_{m3} S \\ &\quad + \epsilon_{r2} \frac{\alpha_{m2}}{\hat{k}_m} \coth \alpha_{m2} d \end{aligned} \quad (9)$$

$$\begin{aligned} G_m(\beta) &= \epsilon_{r3} r_{23} \frac{\alpha_{m3}}{\hat{k}_m} \coth \alpha_{m3} S + \bar{\beta}^2 (1 - r_{23}) \frac{\hat{k}_m}{\alpha_{m3}} \coth \alpha_{m3} S \\ &\quad + \epsilon_{r2} \frac{\alpha_{m2}}{\hat{k}_m} \tanh \alpha_{m2} d \end{aligned} \quad (10)$$

$$T_m(\beta) = \bar{\beta}^2 \left(\frac{\hat{k}_m}{\alpha_{m3}} \coth \alpha_{m3} S + \frac{\hat{k}_m}{\alpha_{m2}} \coth \alpha_{m2} d \right) \quad (11)$$

$$H_m(\beta) = \bar{\beta}^2 \left(\frac{\hat{k}_m}{\alpha_{m3}} \coth \alpha_{m3} S + \frac{\hat{k}_m}{\alpha_{m2}} \tanh \alpha_{m2} d \right) \quad (12)$$

$$Q_m(\beta) = \frac{\hat{k}_m}{\alpha_{m3}} (1 - r_{23}) \coth \alpha_{m3} S \quad (13)$$

$$W_m(\beta) = r_{23} \frac{\hat{k}_m}{\alpha_{m2}} \coth \alpha_{m2} d + \frac{\hat{k}_m}{\alpha_{m3}} \coth \alpha_{m3} S \quad (14)$$

$$R_m(\beta) = r_{23} \frac{\hat{k}_m}{\alpha_{m2}} \tanh \alpha_{m2} d + \frac{\hat{k}_m}{\alpha_{m3}} \coth \alpha_{m3} S \quad (15)$$

$$r_{23} = k_{c2}^2/k_{c3}^2 = (\epsilon_{r2} - \bar{\beta}^2)/(\epsilon_{r3} - \bar{\beta}^2) \quad (16)$$

and $\Delta = QT - PW$ where Q , T , P , W are the limiting values of Q_m , T_m , P_m , W_m for $m \rightarrow \infty$. The functions D_{nm} and K_n are defined in [6]. When the expressions for the unknown constants \bar{r}_1 and \bar{r}_2 , obtained from the appropriate boundary conditions, are substituted in (6) and (7) the following two sets of equations for $\bar{B}_n^{(e)}$, $\bar{C}_n^{(e)}$, $\bar{B}_n^{(h)}$, and $\bar{C}_n^{(h)}$ are obtained:

$$\begin{aligned} &\sum_{m=1}^{\infty} (\hat{k}_p \delta_{pm} - a_m D_{pm} - M_m K_p) \bar{B}_m^{(e)} \\ &\quad + \sum_{m=1}^{\infty} (\hat{k}_p \delta_{pm} - h_m D_{pm} U_m K_p) \bar{C}_m^{(e)} \\ &\quad - \sum_{n=1}^{\infty} (b_n D_{pn} + N_n K_p) \bar{B}_n^{(h)} \\ &\quad - \sum_{n=1}^{\infty} (e_n D_{pn} + V_n K_p) \bar{C}_n^{(h)} = 0, \\ & \quad p = 1, 2, 3, \dots \end{aligned} \quad (17)$$

$$\begin{aligned}
& \sum_{m=1}^{\infty} (c_m D_{qm} + K_q X_{1m}) \bar{B}_m^{(e)} \\
& + \sum_{m=1}^{\infty} (q_m D_{qm} + K_q X_{2m}) \bar{C}_m^{(e)} \\
& - \sum_{n=1}^{\infty} (\hat{k}_q \delta_{qn} - d_n D_{qn} - Y_{1n} K_q) \bar{B}_n^{(h)} \\
& - \sum_{n=1}^{\infty} (\hat{k}_q \delta_{qn} - p_n D_{qn} - Y_{2n} K_q) \bar{C}_n^{(h)} = 0, \\
& \quad q = 1, 2, 3, \dots \quad (18)
\end{aligned}$$

where

$$M_m = a_m \sigma_m \quad N_m = b_m \sigma_m \quad U_m = h_m \sigma_m \quad V_m = e_m \sigma_m \quad (19)$$

$$\sigma_m = - \sum_{q=0}^{m-1} (P_{mq} I_q) / I_h \quad (20)$$

$$X_{1m} = [QM_m I_g - S_{m1} + E_m (Qa_m - Wc_m)] / WI_g \quad (21)$$

$$X_{2m} = [QU_m I_g - S_{m2} + E_m (Qh_m - Wq_m)] / WI_g \quad (22)$$

$$\begin{aligned}
Y_{1m} = & [QN_m I_g - S'_{m1} + E_m (Qb_m - Wd_m) \\
& - (W_m - W) \sin \hat{k}_m a] / WI_g \quad (23)
\end{aligned}$$

$$\begin{aligned}
Y_{2m} = & [QV_m I_g - S'_{m2} + E_m (Qe_m - Wp_m) \\
& - (R_m - R) \sin \hat{k}_m a] / WI_g \quad (24)
\end{aligned}$$

$$S_{m1} = \sum_{n=1}^{\infty} \frac{\sin \hat{k}_n a}{\hat{k}_n} (Q - Q_n) (a_m D_{nm} + M_m K_n) \quad (25)$$

$$S_{m2} = \sum_{n=1}^{\infty} \frac{\sin \hat{k}_n a}{\hat{k}_n} (Q - Q_n) (h_m D_{nm} + U_m K_n) \quad (26)$$

$$S'_{m1} = \sum_{n=1}^{\infty} \frac{\sin \hat{k}_n a}{\hat{k}_n} (Q - Q_n) (b_m D_{nm} + N_m K_n) \quad (27)$$

$$S'_{m2} = \sum_{n=1}^{\infty} \frac{\sin \hat{k}_n a}{\hat{k}_n} (Q - Q_n) (e_m D_{nm} + V_m K_n). \quad (28)$$

The quantities P_{mq} , I_g , I_h , I_q , and E_m are defined in [6].

Equations (17) and (18) together with two equations obtained from the first interface constitute four sets of equations for four sets of unknowns. The rapid convergence property of the coefficients appearing in these equations has been discussed in [6]. Because of this rapidly decaying nature of the coefficients, only a single equation from each set is retained and the desired characteristic equation $F(\beta) = 0$ is obtained from the resulting 4×4 determinant.

III. RESULTS OF COMPUTATIONS

A. Suspended Substrate Shielded Microstrip

In Fig. 2 the dispersion characteristics of the dominant modes of suspended substrate microstrips (SSM's), obtained by solving the lowest order 4×4 matrix equation, are shown together with the dispersion curves of Yamashita and Atsuki [12] for the same set of parameters. The lowest order solution by the present method shows fair agreement with the results of [12] over a wide range of frequencies. The

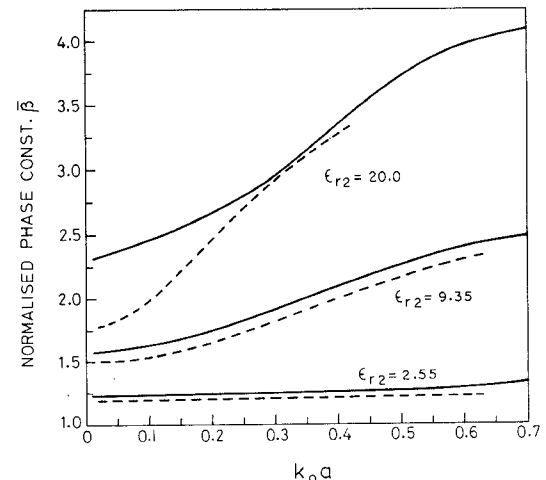


Fig. 2. Dispersion in suspended substrate microstrip (SSM). $\epsilon_{r1} = \epsilon_{r3} = 1.0$. $L/a = b/a = 10$. $S/d_2 = 4.5$. $2a/d_2 = 2.0$. $d/d_2 = 5.5$. —: this method. - - -: Yamashita and Atsuki [12].

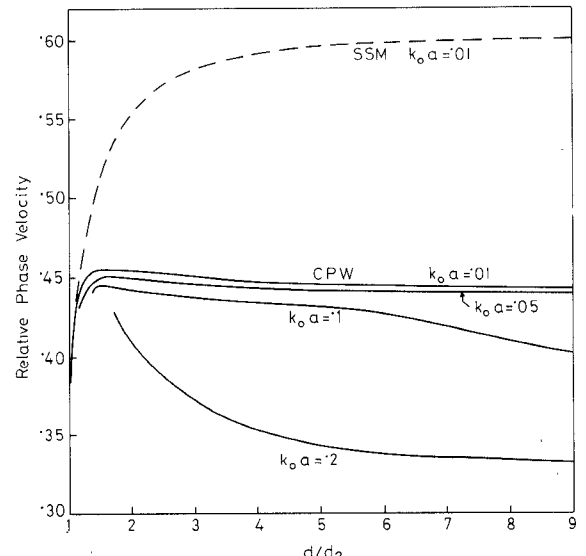


Fig. 3. Variation of relative phase velocity of shielded CPW with d/d_2 for d_2 = slot width = g . $\epsilon_{r1} = \epsilon_{r3} = 1.0$. $\epsilon_{r2} = 10.0$. $a/b = 0.5$. $L/a = 9$. $S/d_2 = 9$. $2a/d_2 = 2$. For SSM, $b/a = L/a = 9$.

agreement, however, is particularly poor for $\epsilon_{r2} = 20$ at the low-frequency end.

B. Shielded Coplanar Waveguide

The dispersion characteristics of shielded coplanar waveguides on alumina substrates were computed for a fixed shape ratio $K = a/b = 0.5$ and three substrate thicknesses, $d_2 = g$, $2g$, and $3g$ where $g = b - a$ = slotwidth. In each case the height of the upper ground plane is $S = 9g$, the box width is $2L = 18g$, and the parameter d/d_2 is varied to change the distance of the bottom ground plane. The results of the computation are presented in Figs. 3-6. For the case $d/d_2 = 1$, when the ground plane is in contact with the substrate, the dispersion curves were computed from a separate program for single-layer substrates. The corresponding equations were obtained from [6] with appropriate modifications to take into account the coplanar ground planes.

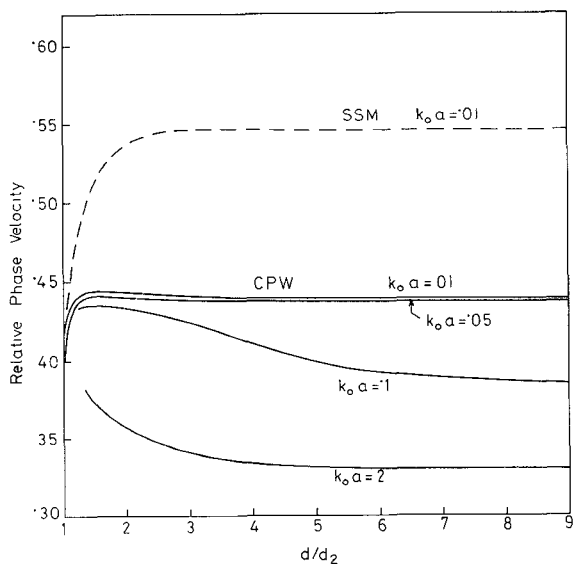


Fig. 4. Variation of relative phase velocity of shielded CPW with d/d_2 for $d_2 = 2$ slot widths = $2g$. $\epsilon_{r1} = \epsilon_{r3} = 1.0$. $\epsilon_{r2} = 10.0$. $a/b = 0.5$. $L/a = 9$. $S/d_2 = 4.5$. $2a/d_2 = 1$. For SSM, $b/a = L/a = 9$.

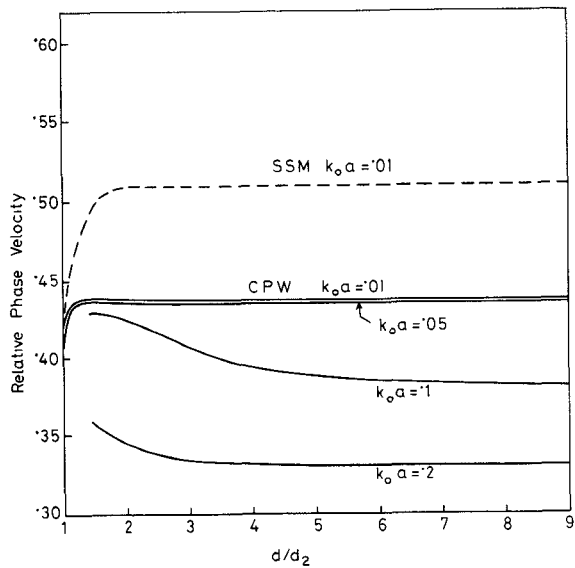


Fig. 5. Variation of relative phase velocity of shielded CPW with d/d_2 for $d_2 = 3$ slot widths = $3g$. $\epsilon_{r1} = \epsilon_{r3} = 1.0$. $\epsilon_{r2} = 10.0$. $a/b = 0.5$. $L/a = 9$. $S/d_2 = 3$. $2a/d_2 = 2/3$. For SSM, $b/a = L/a = 9$.

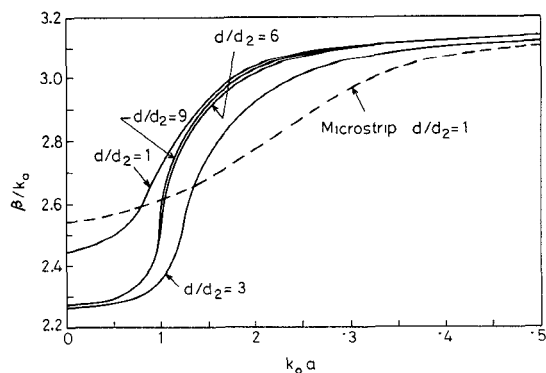


Fig. 6. Normalized dispersion curves of shielded CPW for $d_2 = 2$ slot widths. The parameters are the same as in Fig. 4.

TABLE I

d_2	Open CPW Quasi-TEM \bar{v}_p	Shielded CPW \bar{v}_p	Suspended substrate microstrip \bar{v}_p
g	0.48	0.443	0.600
$2g$	0.45	0.439	0.546
$3g$	0.44	0.436	0.508
∞	0.43	—	—

Note: Substrate Permittivity = 10
 $a/b = 0.5$ for CPW
 $b/a = L/a = 9$ for microstrip
 $d/d_2 = 9$, $k_0a = 0.01$

For an alumina substrate and the particular shape ratio chosen, the results lead to the following observations. For large values of d/d_2 , the relative phase velocity $\bar{v}_p = v_p/c$ becomes independent of the ground plane position, particularly for $d_2 \geq 2g$. For $d_2 = g$, the effect of the ground plane is noticeable even at $d/d_2 = 9$. When $d/d_2 = 1$, the CPW with the ground plane in contact shows preference for the microstrip modes [13]. As the distance of the bottom ground plane is increased, presumably, there is a transition to the CPW modes. One notes that for large d/d_2 the low-frequency \bar{v}_p of the shielded CPW is always lower than that of the corresponding suspended substrate microstrip obtained by removing the coplanar ground planes. It is worthwhile to compare the \bar{v}_p ($k_0a = 0.01$) of CPW with the theoretical quasistatic values of Davies [13] obtained by conformal mapping. This is shown in Table I. The author could not compare his results with Knorr's data [9] for $d_2 = g$ as the frequency parameters in [9] are not normalized.

For $d_2 \geq 2g$ the agreement is good which indicates that for thick substrates the ground plane, when sufficiently far away, should have little effect on quasi-TEM operation. From Fig. 6 one also notes that for $d_2 = 2g$, the CPW dispersion curves are practically identical for large d/d_2 . The agreement is comparatively poor for $d_2 = g$. But the remarkable fact is that the low-frequency \bar{v}_p of the shielded CPW decreases by less than 2 percent as the substrate thickness changes from one to three slot widths, unlike an open CPW, where the corresponding change in quasistatic \bar{v}_p is about 9 percent. Thus it would appear that in a sufficiently large encapsulation, the low-frequency \bar{v}_p of CPW is not much dependent on the substrate thickness in contrast with the open CPW and suspended substrate microstrip as can be seen from Table I.

IV. CONCLUSIONS

The singular integral equation technique has been used to compute the dispersion curves of shielded microstrips on two-layer substrates. From the same analysis it has been possible to obtain a quantitative measure of the effect of metallic encapsulation on CPW. It appears that for alumina with a substrate thickness greater than two slot widths, the ground planes, when sufficiently far away, should have little effect on quasi-TEM behavior.

ACKNOWLEDGMENT

The author wishes to thank P. K. Parua for his help in computation and Prof. B. R. Nag for his kind interest. Thanks are also due to the Computer Centre, University of Calcutta, for providing the computational facilities.

REFERENCES

- [1] C. P. Hartwig, D. Masse, and R. A. Pucel, "Frequency dependent behavior of microstrip," in *Intl. Microwave Symposium (Digest)* (Detroit, MI), May 1968.
- [2] J. S. Hornsby and A. Gopinath, "Fourier analysis of a dielectric loaded waveguide with a microstrip line," *Electron. Letts.*, vol. 5, pp. 265-267, June 12, 1969.
- [3] T. Itoh and R. Mittra, "Dispersion characteristics of slot lines," *Electron. Letts.*, vol. 7, pp. 364-365, July 1971.
- [4] M. K. Krage and G. I. Haddad, "Frequency dependent characteristics of microstrip transmission lines," *IEEE Trans. Microwave Theory Tech.*, vol. MTT-20, pp. 678-688, Oct. 1972.
- [5] E. J. Denlinger, "A frequency dependent solution for microstrip transmission lines," *IEEE Trans. Microwave Theory Tech.*, vol. MTT-19, pp. 30-39, Jan. 1971.
- [6] R. Mittra and T. Itoh, "A new technique for the analysis of the dispersion characteristics of microstrip lines," *IEEE Trans. Microwave Theory Tech.*, vol. MTT-19, pp. 47-56, Jan. 1971.
- [7] D. G. Corr and J. B. Davies, "Computer analysis of the fundamental and higher order modes in single and coupled microstrip," *IEEE Trans. Microwave Theory Tech.*, vol. MTT-20, pp. 669-678, Oct. 1972.
- [8] T. Itoh and R. Mittra, "A technique for computing dispersion characteristics of shielded microstrip lines," *IEEE Trans. Microwave Theory Tech.*, vol. MTT-22, pp. 896-898, Oct. 1974.
- [9] J. B. Knorr and K. D. Kuchler, "Analysis of coupled slots and coplanar strips on dielectric substrate," *IEEE Trans. Microwave Theory Tech.*, vol. MTT-23, pp. 541-548, July 1975.
- [10] H. Hasegawa, M. Furukawa, and H. Yanai, "Properties of microstrip line on Si-SiO₂ system," *IEEE Trans. Microwave Theory Tech.*, vol. MTT-19, pp. 869-881, Nov. 1971.
- [11] H. Guckel, P. A. Brennan, and I. Palocz, "A parallel plate waveguide approach to microminiaturised planar transmission lines for integrated circuits," *IEEE Trans. Microwave Theory Tech.*, vol. MTT-15, pp. 468-476, Aug. 1967.
- [12] E. Yamashita and K. Atsuki, "Analysis of microstrip-like transmission lines by nonuniform discretization of integral equations," *IEEE Trans. Microwave Theory Tech.*, vol. MTT-24, pp. 195-200, Apr. 1976.
- [13] M. E. Davies, E. W. Williams, and A. C. Celestini, "Finite boundary corrections to the coplanar waveguide analysis," *IEEE Trans. Microwave Theory Tech.*, vol. MTT-21, pp. 594-596, Sept. 1973.

Random Discrete Imperfections in Millimeter Waveguide Systems

GABRIELE FALCIASECCA AND SERGIO ROGAI, MEMBER, IEEE

Abstract—A method has been developed to compute the increase of attenuation due to imperfections of finite length randomly distributed in a link. As a limit for the vanishing length the formulas yield the result for random discontinuities. The approach is quite general and can apply to a circular waveguide link as well as to other cases, where the statistics of the problem are described by the power spectrum of the deformation. The applications presented here show how random spacing of the deformations causes significant modifications on the attenuation results; as a particular case some expressions are found to be in agreement with others previously derived. The results are interesting in determining what random variation in the waveguide lengths is sufficient to avoid a serious frequency dependent effect in the attenuation characteristic of a circular waveguide link.

Manuscript received July 19, 1976; revised May 23, 1977. This work was done at Centro Onde Millimetriche of Fondazione Ugo Bordoni under an agreement with Istituto Superiore P. T.

G. Falciasecca is with the Istituto di Elettronica, Università di Bologna, Bologna, Italy.

S. Rogai is with Fondazione Ugo Bordoni, Centro Onde Millimetriche, Bologna, Italy.

I. INTRODUCTION

IN an overmoded circular waveguide link, coupling may arise between the propagating TE₀₁ mode and the other unwanted modes because of many different geometrical imperfections in the guiding structure. Coupling of the TE₀₁ mode with the higher order circular electric modes is the more serious instance of such coupling and can occur because of the presence of mirrors [1], diameter discontinuities at the joints, or the manufacturing process. Attenuation peaks, found experimentally [2], can be attributed to this higher order circular electric mode conversion [3]. In fact discontinuities are always present in a circular waveguide link and eventually are causes of coupling. Diameter variations generate higher order TE_{0n} modes, axis tilts, or offset the TE_{1n} and TM_{1n} modes, etc. Great attention has been devoted to the problem of determining the increase of attenuation due to these discrete random imperfections. Here an approach is presented to compute the solution,